Magnetization Transfer Ratio (MTR) Measurement of Myelofibrosis in Mouse Tibia

version 20211216

I. Executive Summary

The goal of this Co-Clinical Imaging Research Program (CIRP) pre-clinical imaging procedure entitled, "Magnetization Transfer Ratio (MTR) Measurement of Myelofibrosis in Mouse Tibia", is to provide detailed description of key steps used to achieve a stated level of performance embodied in "Claims", for MRI measurement of MTR in mouse tibia of myelofibrosis mouse models. This pre-clinical imaging procedure document will be referred to as a "profile" since it has been designed to have some common features with a Quantitative Imaging Biomarkers Alliance (QIBA) Profile targeting standardization of human quantitative imaging procedures (http://qibawiki.rsna.org/index.php/Main_Page).

Myelofibrosis (MF) is a chronic, ultimately fatal myeloproliferative neoplasm caused by genetic mutations in hematopoietic stem cells leading to systemic inflammation and progressive fibrosis disrupting normal architecture and composition of the bone marrow[1, 2]. Bone marrow biopsy, which is painful and subject to sampling error, remains the default method to assess MF disease in humans. The University of Michigan (UM) CIRP U24 CA 237683 project involves a longitudinal study design in human MF patients and mouse MF models to develop noninvasive quantitative bone marrow MRI methods sensitive to alteration of bone marrow composition due to myelofibrosis evolution and response to MF treatments[3]. The UM CIRP project studies measurement of three image-based metrics (ADC, PDFF, and MTR) that have potential to objectively document MF disease status. Profiles corresponding to ADC and PDFF measurement of MF mouse tibia are also available on the UM CIRP website (UMU24CIRP (umich.edu)). Magnetization transfer imaging is a technique sensitive to magnetization exchange between semi-solid (aka "invisible") and mobile (aka "visible") proton tissue constituents, and potentially has the ability to assess fibrosis due to increased collagen [4, 5]. Normal bone contains red marrow where red blood cells, platelets and white blood cells are created, and yellow marrow that contains fat [6-8]. This document details procedures for MTR measurement in MF mouse tibia to achieve stated performance claims. Here we treat MTR as a "quantitative" metric, although numerical MTR results are a strong function of multiple experimental parameters and MRI hardware conditions. In reality in our context, MTR is relative metric, and we do not claim to measure absolute MTR values. This profile will adopt the common practice to express MTR values in "% units" on 0 to 100% scale. Empirically, MTR reflects percentage of visible signal loss due to application of off-resonance saturation RF energy depleting magnetization in the semi-solid (invisible) macromolecular matrix thus reducing magnetization replenishing visible signal. Simple fluids free of macromolecules should have an MTR ≈ 0%, whereas macromolecule-rich semi-solid tissues such as myelin, muscle, scar and collagen exhibit relatively high MTR (>50%). Interestingly, simple fats exhibits very low MTR.

II. Pre-Clinical Imaging Claims

Tibia bone marrow composition in MF mouse models has gradation going from proximal to distil ends of the tibia, therefore separate claims are made for volume of interest (VOI) analysis of MTR maps for each of three distinct sections along the length of the tibia (see Figure 1):

Section 1 (proximal) ≡ VOI (4-5mm^3) within 7mm of proximal end of tibia
Section 2 (transition) ≡ VOI (0.4-0.5mm^3) from 8 to 10mm of proximal end of tibia
Section 3 (distil) ≡ VOI (0.1-0.2mm^3) from 11 to 12mm of proximal end of tibia

Claim 1: A measured change in the mean MTR in Section 1 VOI of MF mouse model tibia that exceeds ±16% indicates a true biological change has occurred in the tibia bone marrow with 95% confidence.

Claim 2: A measured change in the mean MTR in Section 2 VOI of MF mouse model tibia that exceeds ±11% indicates a true biological change has occurred in the tibia bone marrow with 95% confidence

Claim 3: A measured change in the mean MTR in Section 3 VOI of MF mouse model tibia that exceeds ±9% indicates a true biological change has occurred in the tibia bone marrow with 95% confidence

The claims hold when:

- **Scanner hardware, 3D FLASH acquisition method and parameters, image reconstruction, and data-reduction procedures are equivalent (or superior) to those detailed in section III.**
- **Use of the same animal model and interventions to induce myelofibrosis are performed as detailed in section IV.**
- **MTR change is assessed on an individual animal basis where each animal undergoes identical procedures on the same MRI system over longitudinal timepoints.**

III. MR Imaging Process Specifications

1. MRI Scanner Hardware
    i. Bruker BioSpec® MRI Console Paravision 7.0.0 software installed on 64 bit Linux multicore workstation, 16 GB RAM, 1TB hard disk.
    ii. 7Tesla, 30cm bore magnet model “7T/310/AS” System (Agilent) with compact Faraday RF-shielding cabinet is attached to the magnet service end
    iii. System gradient/shim coil set model “B-GA12S HP” with standard 300V/200A gradient amplifier and standard 5A shim amplifier:
        a. Inner diameter 114mm
        b. Gradient strength 440 mT/m

c. Max slew rate 3,440 T/m/s
d. 10 shim channels, up to 4th order shim coils

iv. Large Transmit/Receive RF Volume Coil: Outer/inner diameter 112mm/86mm
v. Medium Transmit/Receive RF Volume Coil: Outer/inner diameter 75mm/40mm RF RES 300 1H 075/040 QSN TR; model 1P T13161V3.
vi. Small Receive: CryoProbe™ 4 Element Array RF Coil Kit for Mice cryogenically cooled to 20-30°K with parallel receiver upgrade.

2. Acquisition Technique
   i. Magnetization transfer sequence was gradient-echo 3D "Method=<Bruker:FLASH>".
   ii. Two consecutive 3D FLASH series were acquired, one *WITHOUT* additional off-resonance RF saturation pulse ("MToff"), and one *WITH* an additional gauss-shaped, 8μT amplitude, 100ms duration RF saturation pulse -2400Hz off-resonance ("MTon").
   iii. Hardware settings, acquisition geometry, shim, transmit gain and receiver gains were held constant over the 2 consecutive series such that change in signal is measurable by simple subtraction of MTon from MToff images, assuming the spectrometer is stable.
   iv. Magnetization transfer sequence was 3D FLASH in coronal plane with geometry:

Table I: 3D FLASH geometry

Matrix	Acquired Voxel Size (μm)	FOV (mm)
256 (freq enc on z-axis)	90 on z	23.04 on z
128 (phase enc on x-axis	75 on x	9.6 on x
64 (phase enc on y-axis)	94 (slice thickness) on y	6.0 on y

   v. Contrast Control: single-echo; TR/TE=111ms/2.99ms; flash-spoiling, Flip angle = 9°; 1 NSA. Two series total scan time = 15min x 2 = 30min.
   vi. Conventional 3D sequential cartesian k-space trajectory, 1 phase-encode / TR.
   vii. Full k-space acquisition, no acceleration, no multi-band, no turbo spin-echo.
   viii. No physiologic synchronization. Anesthetized mouse leg is held in place between 3D-printed, leg-shaped mold on posterior side and CryoProbe™ on anterior side.

3. Image Reconstruction
   i. Time-domain 3D FLASH data are reconstructed to magnitude-valued space-domain on the Bruker MRI system using standard 3DFT image reconstruction routines within the Paravision 7.0.0 environment. Three-D images for MToff and MTon series are stored "pdata" data tree in "2dseq" datafile format. Associated Bruker-generated text files "acqp", "AdjStatePerScan", "configscan", "method", "pulseprogram", "specpar", "id", "methreco", "procs", "reco", and "visu_pars" are stored in series-level folders within the exam-level folder. Exam-level folders, coded by group+mouseID+acqdate+acqtime, are transferred to UM-maintained drives for archival and subsequent analysis described below.

4. Biomarker Map Generation
    i. Conversion from Bruker 3D FLASH magnitude-valued 2dseq-format to MTR-related ITK-compatible format images is performed using a custom MATLAB (ver ≥2016b) "ProcessLegTLC.m" script that calls scripts within Bruker-provided "pvmatlab" (ver 2013) MATLAB package for handling ParaVision data.
    ii. Initially, ProcessLegTLC surveys all "method" text files for parameter values of keywords to create a catalog of the entire exam. The catalog is stored in a "GroupID_MouseID_DateTime_Catalog.tsv" text file containing key attributes for each series: [Series#; ScanTime; Protocol; Method; TR; TE; NEcho; Nave; PVM_Matrix; Thk; Nslc; MTsatFreq; MTstate; Receiver_Gain; ReconSize; bvalue].
    iii. Series cataloged with keyword "Protocol" = "FLASH3D_MT_OFF" and "FLASH3D_MT_ON", read for calculation of MTR defined for pixels having SNR≥20:

$$MTR = 100\% \cdot \frac{(MToff - MTon)}{MToff}$$

    iv. Pixels below this SNR threshold are set to 0. MTR, MToff and MTon were stored on disk as 3D images in ITK-compatible MetaImage format comprised of paired header (eg. "ABCD.mhd") and binary data (eg. "ABCD.raw"). MetaImage format 3D volumes provide compactness and portability to commonly used medical/scientific image viewing platforms, such as ITK-SNAP and 3DSlicer. Geometry content (slice location, extent and angulation) are retained in the mhd header structure.

5. Additional Map Conditioning

    Data reported in this profile *DID NOT* undergo additional conditioning beyond that detailed in sections 6 through 9 below. However, spatial registration of image volumes will be performed in UM CIRP U24 CA 237683 study of MF in mouse tibia to longitudinally follow disease evolution and response to treatment. For completeness, the process for spatial registration of a mouse tibia over time is described below:
    i. MATLAB scripts with a GUI interface were developed in the UM Center for Molecular Imaging (CMI) to facilitate MATLAB calls to Elastix (ver 4.8) image registration software (elastix: download (lumc.nl)). This tool was designed to input/output MetaImage format 3D volumes as created by ProcessLegTLC script.
    ii. In addition to multi-slice MTR-related images, the MF tibia MRI protocol includes a variety of imaging contrasts including: DWI-related (DWIb0) and PDFF-related (MGEmean) images. The 3D MToff is used as the reference "FIXED" image volume to which other DWIb0 and MGEmean, are called "MOVERs", which are spatially transformed to spatially align with the FIXED volume.
    iii. The tibia is effectively a rigid body, whereas surrounding muscle may be deformed over serial MRI sessions. Therefore, the tibia is manually segmented on the FIXED image baseline timepoint using the CMI GUI (or 3DSlicer) and saved in MetaImage format. A dilated version of the tibia VOI segmentation

serves as a mask to drive the Elastix rigid-body volume registration routine based on tibia anatomic features without regard to muscle features.

iv. The CMI GUI prompts user to identify 4 points on the FIXED tibia along with 4 homologous points on the MOVER tibia to initialize the Euler (rigid body) transformation. For this step, two landmarks on the distil end of the tibia and two mid-tibia are used.

v. Main Elastix parameters are:
   a. FIXED = "*_MT_Off.mhd"
   b. MOVER = "*_MGEmean.mhd"
   c. MASK = "*_MT_Off_VOI.mhd"
   d. Sample: RandomSparseMask
   e. Metric: Mutual Information
   f. Transform: Euler
   g. Final Interpolation: BSpline-3
   h. Iterations: 4000
   i. NSamples: 5000

vi. Complete Elastix parameter file is provided in Appendix I. Since all MT-related, DWI-related and PDFF-related 3D images all have identical acquisition geometry, the final spatial transformation that aligns them to the fixed reference is applied to the other like-related 3D volumes. All spatially registered volumes are output to disk with their original filename amended by an "_R". Elastixlog.txt, ElastixParameters.txt, and TransformParamters.txt are also retained in sub-folders for future use.

6. Region / Volume of Interest (ROI / VOI) Segmentation

i. For longitudinal datasets spatially-registered to common (FIXED) dataset, the original tibia segmentation saved in "*_MT_Off_VOI.mhd" may be applied to any co-registered datasets. This *WAS NOT DONE* nor was it necessary for data, analysis and results reported in this profile.

ii. For this profile reporting repeatability of MTR measurement in MF mouse tibia using Test-retest design, the tibia was manually segmented independently for each Test and ReTest dataset. Also note, the CMI GUI or other 3D image analysis platform such as 3DSlicer may be used to manually segment tibia with the resultant output stored in MetaImage format with "*_VOI.mhd" filename. For this profile, both Test and ReTest datasets from all mice and timepoints were manually segmented using the CMI GUI by one individual (KH).

iii. Gradation in MTR from proximal to distil ends of the tibia was dealt with by separate analysis of three sections along the length of the tibia, each with its own repeatability claim.

iv. To systematically define these sections, a dedicated MATLAB script was created to read-in the VOI mask and automatically detect a landmark (knee) defined as the Z-slice containing largest VOI cross-section in X-Y plane. Then given known slice thickness, three sections were parsed by Z-dimension from the VOI as displayed in Figure 1 and defined as:

Section 1 (proximal) ≡ VOI (4-5mm^3) within 7mm of proximal end of tibia
Section 2 (transition) ≡ VOI (0.4-0.5mm^3) from 8 to 10mm of proximal end of tibia
Section 3 (distil) ≡ VOI (0.1-0.2mm^3) from 11 to 12mm of proximal end of tibia

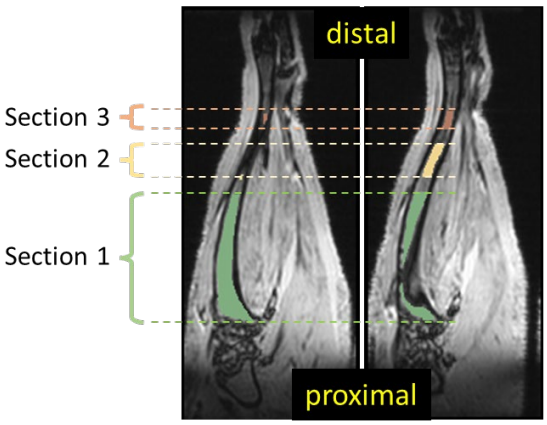

Figure 1: Sections 1,2,3 derived from 3D VOI mask are systematically defined at pre-set distances from proximal end of tibia. Two coronal slices are shown to better display extent of all three sections.

v. High fat-content and low SNR zones can lead to unreliable, or even negative MTR values (Figure 2). In effort to limit impact of poor quality data, a threshold VOI mean MTR value of +10% was applied. That is, VOI mean MTR had to be ≥10% on both test and retest scan dates to be included in test-retest analysis. Sections 1, 2, and 3 were analyzed independently, though all used the same MTR ≥10% acceptance threshold.

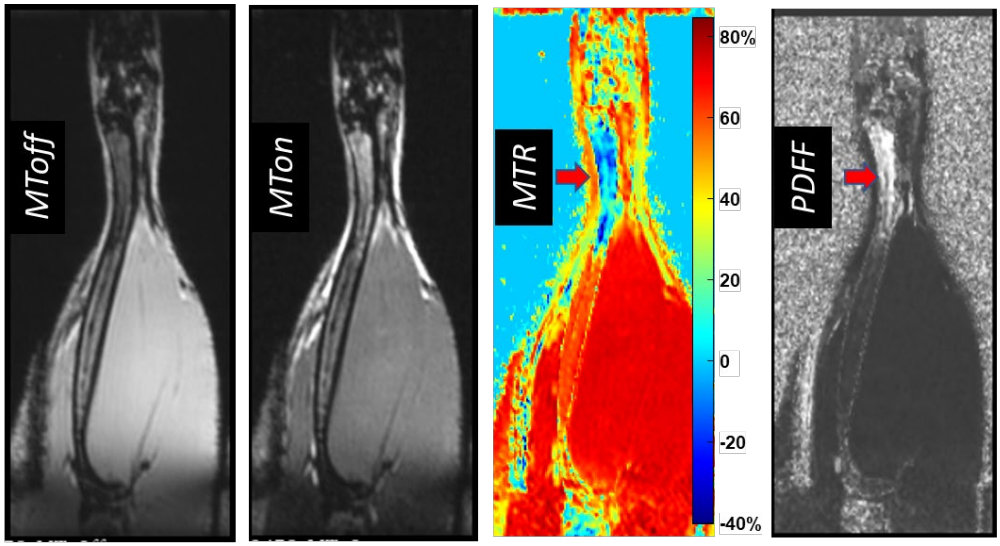

Figure 2: Less reliable MTR calculation in low SNR and high fat-content zones. MTR is shown in pseudo-color to better see non-physical negative MTR values that may occur in high PDFF (red arrows) tissues.

7. Biomarker Metric
   i. Three-D masks for Sections 1, 2, and 3 were applied independently to MTR maps. The mean MTR of voxels within each mask is taken as the "biomarker".

Repeatability of mean MTR for each section was analyzed by test-retest study design where MF model mice were scanned on two consecutive days where biological change in the tibia over 1 day is expected to be small/insignificant.

8. Imaging System Performance Validation
    i. Magnetization transfer is sensitive to magnetic field and transmit RF field uniformity. The UM CIRP MF project is required to measure MTR in mouse tibia which is ~17mm long with ~0.8mm diameter. Magnetization transfer fraction (MTF) material labeled "MTF14" was made by adding 14g of solid material to 100g of lactate water. The solid fraction is composed of 69% cetearyl alcohol, 17% BTAC (behentrimonium choride), and 14% SAPDA (stearamidopropyl dimethylamine) by weight. A simple MTR phantom was constructed within a 10mm diameter test tube to contain 2mm and 0.5mm diameter capillary tubes filled with MTF14 (high MT contrast) and 50% polyvinylpyrrolidone that exhibits ADC contrast but no MT. The surrounding media was 40% PVP material. The MTF14 and PVP50 materials were loaded in both 2mm and 0.5mm diameter capillaries to confirm that measured values in small tube and large tubes agree and is uniform over the length of mouse tibia along z-axis. Per Figure 3, MTR values in the 0.5mm diameter capillary are within 3% of the large capillary, and can be expected to be reasonably uniform over the length of a mouse tibia.

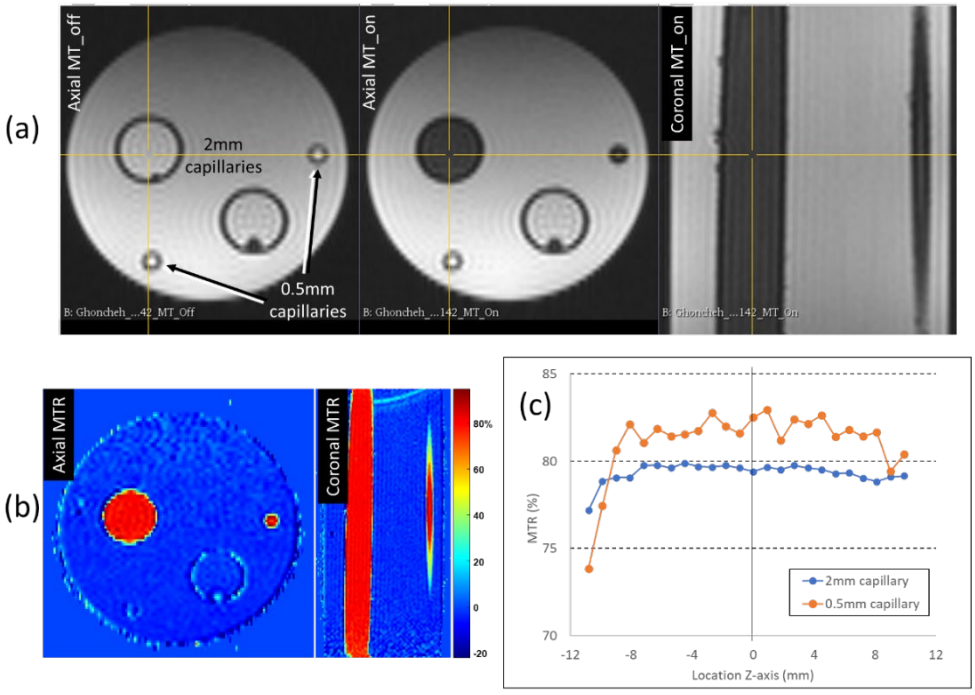

Figure 3: (a) MT_off and MT_on in axial and coronal views of MTR phantom. (b) MTR map indicates MTF14 material has high MT properties, as apparent in top 2mm and 0.5mm capillary tubes, and PVP that does not exhibit MT in bottom capillaries. (c) Graph shows slight overestimation of MTR in small capillary relative to large capillary likely due to edge effects. MTR values are uniform over central 16mm extent along z-axis.

9. Statistical methods and data supporting claim(s)
    i. Repeatability of VOI mean MTR in MF mouse tibia was assessed using a "test-retest" design study [9, 10].
    ii. A total of 15 female BALB/c JAK2 mutant MF model mice were included in this study. MF disease model was induced by whole body irradiation to ablate bone marrow, followed by same day bone-marrow transplant (BMT) a 50% - 50% combination of normal and diseased cells per the protocol summarized in Section IV below. MTR mapping was performed over 4 to 10 weeks following BMT as the disease developed in the marrow space. Each test-retest MTR dataset pair was acquired on two consecutive days for each animal, followed by 9 to 14 days without MRI. Typically, test-retest pairs were spaced 10 to 14 days apart, such that a total of 37 test-retest pairs were collected from these 15 mice. Since the disease develops relatively slowly over the 10 weeks following BMT, the biological status of bone marrow over any given 24 hour period (i.e. a test-retest pair) is assumed to be effectively constant. Moreover, while correlation between pairs from a given animal is possible, the 37 test-retest pairs were treated as independent measurements to simplify analysis.
    iii. To limit artifactual data in the analysis, if VOI mean MTR was below 10% for either test or retest datasets, the pair was excluded. VOIs from Sections 1,2 and 3 were independently screened for the MTR < 10% rejection threshold.
    iv. Explicit steps to assess repeatability followed Bland-Altman and QIBA-recommended procedures summarized as [9-11]:
        a. Calculate mean (M) and variance (V) for each test-retest pair

$$M = \frac{(MeanPDFF_{test} + MeanPDFF_{retest})}{2};$$
$$V = \frac{(MeanPDFF_{test} - MeanPDFF_{retest})^2}{2}$$

        b. For each of N-pairs, calculate $V/(M^2)$, take the mean over all N-pairs, then take square root to get within-subject coefficient of variation, wCV (in % units):

$$wCV = 100\% \cdot \sqrt{\frac{1}{N}\sum_i^N \frac{V_i}{M_i^2}}$$

        c. Note, wCV is a relative (dimensionless) repeatability metric that becomes unreliable as M→0. For non-relative repeatability of PDFF, we use within-subject standard deviation, wSD, and repeatability coefficient, RC given by:

$$wSD = \sqrt{\frac{1}{N}\sum_i^N V_i}$$
$$RC = 2.77 \cdot wSD$$

        d. The RC is a measure of precision and useful to infer minimum threshold of observed biomarker change attributable to true biologic change (with 95% confidence), as opposed to measurement error.

e. The corresponding 95% confidence interval (α = 0.05) to RC are given by multiplicative lower-bound (LB) and upper-bound (UB) factors given by ChiSqr function for N-1 degrees of freedom [9, 10]:

$$95\%\ CI\ of\ RC = RC \cdot \left[\frac{1}{\sqrt{(N-1)\cdot\ \chi^2_{0.975}}};\ \frac{1}{\sqrt{(N-1)\cdot\ \chi^2_{0.025}}} \right]$$

f. The same multiplicative LB and UB factors were used to estimate 95% CI's for wCV and wSD. Test-retest results are summarized in Table II:

Table II	Section 1	Section 2	Section 3
N Test Retest Pairs	37	28	22
Mean MTR (%)	57.6	37.4	22.4
Bias (MTRretest – MTRtest) (%)	-2.2	+0.6	+2.6
wCV [LB, UB] (%)	11.7 [9.5, 15.2]	17.4 [13.8, 23.7]	14.3 [11.2, 20.8]
wSD [LB, UB] (%)	5.7 [4.6, 7.4]	3.9 [3.0, 5.2]	3.4 [2.6, 4.8]
RC [LB, UB] (%)	15.7 [12.8, 20.4]	10.7 [8.4, 14.5]	9.3 [7.2, 13.3]

g. Bland-Altman x-y plots provide a graphic view of repeatability [11], where x = (MTR_{retest} + MTR_{test})/2 and y = (MTR_{retest} - MTR_{test}). Mean of y is a measure of bias (dotted line), or apparent MTR change between test and retest conditions. Ideally, bias is close to zero thereby supporting the assumption that bone marrow was biologically constant between test and retest measurements. Dashed lines (bias ± 1.96*SD) provide a graphical indication of measurement precision.

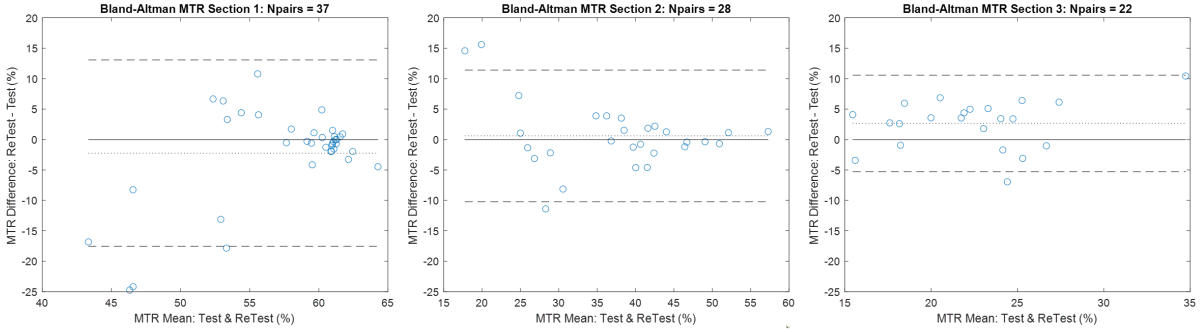

Figure 4: Bland-Altman plots of MTR Test-Retest in mouse tibia Sections 1 (left); Section 2 (middle); and Section 3 (right) all shown on same vertical scale to illustrate different variability in Sections 1, 2 and 3. Relative to Section 1, Sections 2 and 3 have lower MTR due to more fat.

IV. Animal Model Specifications

1. Species: mouse
2. Strain: C57BL/6.
3. Sex: Female
4. Age at start of data acquisition: ~12 weeks
5. Disease induction:
    i. The JAK2 V617F ($JAK2^{+/VF}$) animal model of myelofibrosis (MF) was generated using resultant 8-10 week old female donor offspring from cross between $JAK2^{+/VF}$ mice (B6N.129S6(SJL)-*Jak2*$^{tm1.2Ble}$/AmlyJ; Charles River Stock No. 031658) and Mx-Cre mice (B6.Cg-Tg(Mx1-cre)1Cgn/J; Charles River Stock No. 003556), similar to previously described methods [12, 13].
    ii. Whole bone marrow cells were isolated from $JAK2^{+/VF}$ donor mice and mixed 1:1 with whole bone marrow cells isolated from wild-type mice.
    iii. A total of 1×10^7 bone marrow cells mixed 1:1 were injected retro-orbitally into lethally irradiated 6-8 week old female C57BL/6 recipient mice.
    iv. Polyinosinic-polycytidylic acid (10 mg/kg) was administered intra-peritoneally 10 days post-bone marrow transplant (post-BMT).
    v. Development of MF was evaluated by spleen volumes using MRI beginning 4 weeks post-BMT, continuing every 2 weeks thereafter.
6. Therapeutic intervention – Not Applicable
7. Animal prep and during imaging: 1.5% Isofluorane/air inhalation
8. Animal monitoring/support during imaging:
    i. Thermoregulated heating bed during imaging
    ii. Respiratiory montoring (SAI monitor)
9. Animal recovery: isolated cage until full recovery, then back to communal cage
10. Imaging schedule: Each test-retest MTR dataset pair was acquired on two consecutive days for each animal starting ~28 days post-BMT. Test-retest pairs were spaced approximately 10 to 14 days apart, such that a total of 37 test-retest pairs were collected from 15 mice.

V. Outcome Specifications

1. Time to moribund/survival
2. Longitudinal body weight and spleen volume measurements (last MRI) and spleen weight at sacrifice
3. Tibia and spleen tissues were harvested for flow cytometry and histological analysis
    i. Complete Blood Count (CBC); flow cytometry for immune cell populations
    ii. Liver and spleen weight
    iii. Liver, spleen and femur/tibia histology preparation and staining
    iv. Immune cell populations of spleen and bone marrow
    v. Immuno-blotting of spleen tissue

References

1. Garmezy, B., et al., *A provider's guide to primary myelofibrosis: pathophysiology, diagnosis, and management.* Blood Rev, 2021. **45**: p. 100691.
2. Schaefer, J.K., et al., *Primary myelofibrosis evolving to an aplastic appearing marrow.* Clin Case Rep, 2018. **6**(7): p. 1393-1395.
3. Luker, G.D., et al., *A Pilot Study of Quantitative MRI Parametric Response Mapping of Bone Marrow Fat for Treatment Assessment in Myelofibrosis.* Tomography, 2016. **2**(1): p. 67-78.
4. Knutsson, L., et al., *CEST, ASL, and magnetization transfer contrast: How similar pulse sequences detect different phenomena.* Magn Reson Med, 2018. **80**(4): p. 1320-1340.
5. Martens, M.H., et al., *Magnetization transfer ratio: a potential biomarker for the assessment of postradiation fibrosis in patients with rectal cancer.* Invest Radiol, 2014. **49**(1): p. 29-34.
6. Bani Hassan, E., et al., *Bone Marrow Adipose Tissue Quantification by Imaging.* Curr Osteoporos Rep, 2019. **17**(6): p. 416-428.
7. Li, X. and A.V. Schwartz, *MRI Assessment of Bone Marrow Composition in Osteoporosis.* Curr Osteoporos Rep, 2020. **18**(1): p. 57-66.
8. Rosen, C.J., et al., *Marrow fat and the bone microenvironment: developmental, functional, and pathological implications.* Crit Rev Eukaryot Gene Expr, 2009. **19**(2): p. 109-24.
9. Raunig, D.L., et al., *Quantitative imaging biomarkers: a review of statistical methods for technical performance assessment.* Stat Methods Med Res, 2015. **24**(1): p. 27-67.
10. Winfield, J.M., et al., *Extracranial Soft-Tissue Tumors: Repeatability of Apparent Diffusion Coefficient Estimates from Diffusion-weighted MR Imaging.* Radiology, 2017. **284**(1): p. 88-99.
11. Bland, J.M. and D.G. Altman, *Statistical methods for assessing agreement between two methods of clinical measurement.* Lancet, 1986. **1**(8476): p. 307-10.
12. Mullally, A., et al., *Physiological Jak2V617F expression causes a lethal myeloproliferative neoplasm with differential effects on hematopoietic stem and progenitor cells.* Cancer Cell, 2010. **17**(6): p. 584-96.
13. Stivala, S., et al., *Targeting compensatory MEK/ERK activation increases JAK inhibitor efficacy in myeloproliferative neoplasms.* J Clin Invest, 2019. **129**(4): p. 1596-1611.

Appendix I: Elastix Parameters (automatically retained in “ElastixParameters.txt” file)

```
(FixedInternalImagePixelType "float")
(FixedImageDimension  3)
(MovingInternalImagePixelType "float")
(MovingImagedimension  3)
(UseDirectionCosines "false")
(WriteTransformParametersEachIteration "false")
(WriteTransformParametersEachResolution "true")
(WriteResultImageAfterEachResolution "false")
(WriteResultImage "true")
(Registration "MultiResolutionRegistration")
(Metric "AdvancedMattesMutualInformation")
(UseJacobianPreconditioning "false")
(FiniteDifferenceDerivative "false")
(ShowExactMetricValue "false")
(UseFastAndLowMemoryVersion "false")
(NumberOfHistogramBins  32)
(NumberOfFixedHistogramBins  32)
(NumberOfMovingHistogramBins  32)
(FixedLimitRangeRatio  0)
(MovingLimitRangeRatio  0)
(FixedKernelBSplineOrder  1)
(MovingKernelBSplineOrder  3)
(ImageSampler "RandomSparseMask")
(NumberOfSpatialSamples  5000)
(NewSamplesEveryIteration "true")
(UseRandomSampleRegion "false")
(CheckNumberOfSamples "true")
(Interpolator "LinearInterpolator")
(ResampleInterpolator "FinalBSplineInterpolator")
(FinalBSplineInterpolationOrder  3)
(Resampler "DefaultResampler")
(ResultImageFormat "mhd")
(ResultImagePixelType "float")
(ErodeFixedMask "false")
(ErodeMovingMask "false")
(DefaultPixelValue  0)
(Transform "EulerTransform")
(AutomaticTransformInitialization "false")
(AutomaticScalesEstimation "true")
(HowToCombineTransforms "Compose")
(Optimizer "StandardGradientDescent")
(NumberOfSamplesForSelfHessian  100000)
(NumberOfGradientMeasurements  0)
```

```
(NumberOfJacobianMeasurements  2700)
(NumberOfSamplesForExactGradient  100000)
(MaximumNumberOfIterations  4000)
(MaximumNumberOfSamplingAttempts  0)
(SP_a  2)
(SP_alpha  0.60200000)
(SP_A  50)
(NumberOfResolutions  1)
(FixedImagePyramid "FixedSmoothingImagePyramid")
(FixedImagePyramidSchedule  1  1  1)
(MovingImagePyramid "MovingSmoothingImagePyramid")
(MovingImagePyramidSchedule  1  1  1)
(Scales  10000  10000  10000  1  1  1)
```